

2 mm waveband saturation transfer electron paramagnetic resonance of conducting polymers

V. I. Krinichnyi^{a)}

Institute of Problems of Chemical Physics, RAS, N.N. Semenov Avenue 1, Chernogolovka 142432, Russia

(Received 7 April 2008; accepted 12 August 2008; published online 6 October 2008)

The 2 mm waveband (140 GHz) saturation transfer electron paramagnetic resonance (ST-EPR) spectroscopy has been employed to characterize the very slow microsecond to millisecond librational macromolecular dynamics of a wide range of conducting polymers. It is possible at this waveband to determine separately spin relaxation and dynamics affecting ST-EPR spectra. Higher microwave frequency provides substantial increases sensitivity of the method to the anisotropic macromolecular motion in conducting polymers and broadens the interval of correlation times up to 1–80 ms, thereby extending the slow-motion limit for ST-EPR by two orders of magnitude compared with convenient wavebands EPR. © 2008 American Institute of Physics.

[DOI: 10.1063/1.2977991]

I. INTRODUCTION

Conducting polymers (CPs) with a highly anisotropic quasi-one-dimensional (Q1D) π -conjugated structure are of great interest both for fundamental research and for their perspective applications in molecular electronics.^{1,2} In contrast to such traditional systems as silicon, polyethylene, etc., the conductivity of such systems can be controlled by their chemical or electrochemical oxidation or reduction from insulator state to semiconductor and then to metal ones. The charge in CPs is transferred by nonlinear topological distortions, polarons, and solitons, characterized by spin $S = \frac{1}{2}$ and high Q1D mobility along polymer chains. The charge can also hop between these carriers moving along neighboring polymer chains, which is a reason for the highly anisotropic conductivity of CPs. Such peculiarities of CPs cause their fundamentally unique magnetic and electronic properties.

Both the intra- and interchain charge transfers in CPs correlate with their structure, morphology, and ordering.^{3,4} Moreover, the transverse integral is modulated by superslow fluctuations of their lattice oscillations^{5,6} which, in turn, depend on the system crystallinity or dimensionality. Polymer chains *a priori* librate with microsecond correlation time τ_c .^{7,8} Such processes are studied by the saturation transfer electron paramagnetic resonance (ST-EPR) spectroscopy first developed for the study of various condensed systems (glasses, crystals, polymers, and biological systems) modified by stable paramagnetic centers (PCs), normally, nitroxide radicals, with anisotropic magnetic parameters.^{9,10} ST-EPR expanded considerably the spin label and probe method in the study of molecular dynamics in polymers with $10^{-7} \text{ s} \leq \tau_c \leq 10^{-3} \text{ s}$, inaccessible for convenient, linear on the microwave (MW) field, EPR spectroscopy.^{8,11,12}

The method is found in an analysis of the complementary first-harmonic dispersion (U_1^1) or second-harmonic ab-

sorption (V_2^1) spectra detected in the phase quadrature ($\pi/2$ -out-of-phase) with the field modulation on the microwave field B_1 when the adiabatic saturation condition is fulfilled. However, these terms of ST-EPR signal possess a complex dependency on a great number of parameters. Besides, the parameters of molecular motion which is normally anisotropic in condensed media cannot be determined directly from the analysis of a line shape of the 3 cm waveband (X band at $\omega_e/2\pi \approx 10 \text{ GHz}$ and $B_0 \approx 3.3 \text{ kG}$) ST-EPR spectrum^{13,14} due to a low spectral resolution and the interferential effect of relaxation processes on a signal shape. It is important to note that the rotation of PCs with a correlation time τ_c and their relaxation on the lattice phonons with a spin-lattice relaxation time T_1 differently effect an effective ST-EPR spectrum shape. Indeed, the spectral diffusion, stipulated by spin reorientation with correlation time τ_c , is proportional to the steepness of the magnetic field change $dB(\vartheta)/d\vartheta$ (here, ϑ is the angle between an external magnetic field \mathbf{B}_0 and a radical main axis); i.e., even in the case of isotropic rotation it is not the same in distinct spectrum ranges, while spin-lattice relaxation, provided that it does not depend on orientation, is the same for all regions of the spectrum. This is why the inequalities $\Delta\omega\tau_c \gg 1$, $100T_1 > \tau_c > 0.01T_1$ should be fulfilled for the region of their superslow tumbling domain. The first inequality shows that the absorption EPR spectrum is the same as that obtained by using a rigid powder. The second inequality leads to a spectral diffusion of saturation across the spectrum, since rotational diffusion is comparable to T_1^{-1} . This inequality is valid for PCs characterizing by comparatively high spin-orbit coupling and correlation time changing within the above range. Therefore, the main problems of the method are the separation of the effects of magnetic relaxation and anisotropic molecular motion onto the ST-EPR spectrum shape.

Certain perspectives of ST-EPR method improvement can be expected with the increase of registration frequency.⁹ This should improve the spectral resolution, i.e., simplify the spectral structure, and increase the spectral diffusion rate,

^{a)} Author to whom any correspondence should be addressed. Electronic mail: kivi@cat.icp.ac.ru.

which depends on the registration resonant frequency ω_e . As the g factor of stable organic PCs with heteroatoms is anisotropic, the spectral resolution of the components of their EPR spectra can be enhanced by increasing the registration frequency ω_e , i.e., $\Delta\omega \propto \Delta g = g_{ii} - g_e \propto \omega_e$ (here, $g_e = 2.00232$ is the g factor for free electron). Besides, the sensitivity of the ST-EPR method to molecular motion is enhanced quadratically with the anisotropy of magnetic parameters⁹ and approximately linearly on the effective T_1 .¹⁵ This should also lead to the increase in the MW saturation velocity along a spectrum which is proportional to the slope square of resonant field on a rotation angle⁹ as well as in the sensitivity of EPR method, i.e., minimum number of the registering spins N_{\min} .¹⁶ Indeed, the calculation of the ST-EPR spectra of anisotropic diffusing PCs showed¹³ that the transition to the 8 mm waveband (Q band at $\omega_e/2\pi \approx 35$ GHz and $B_0 \approx 12.5$ kG) EPR increases the sensitivity of ST-EPR spectra to the anisotropy of molecular rotation. At this waveband EPR, however, the anisotropy of a resonant field of nitroxide radicals due to the g tensor becomes comparative with the anisotropy of superfine interaction. This is a reason why the lines of different canonical orientations remain not resolved. Therefore, the literature concerning the effect of the motion of π conjugated chains onto interchain charge transfer is sparse and no significant progress has been achieved in this field up to today.

Earlier we have shown^{17–20} that the measurement of organic radicals in different solids, especially in conducting polymers at the 2-mm waveband (D band at $\omega_e/2\pi \approx 140$ GHz and $B_0 \approx 50$ kG) enables us to increase considerably the absolute sensitivity, precision, and informativity of the method. At high frequencies the main advantage of the “linear” method is the higher spectral resolution of the g factor that expands by more than an order of magnitude the range of fast molecular motions in condensed systems. High spectral resolution allows independent analysis of the relaxation change in all main radical orientations in an external magnetic field that increases considerably the descriptiveness of the “linear” EPR spectra in the study of anisotropic molecular rotations. Besides, the minimum number of spins detected, increases with the increase of ω_e as $N_{\min} \propto \omega_e^{-\alpha}$, where $\alpha \approx 0.5–4.5$.¹⁶ Finally, the probability P_{cr} of cross-relaxation of PCs decreases strongly with the increase of a polarizing MW quantum energy $h\omega_e \propto B_0$ as $P_{\text{cr}} \propto \exp(-B_0^2)$,²¹ so the spin packets become noninteracting at D -band EPR and, therefore, can be saturated at lower values of the magnetic term B_1 of the polarizing MW field. The electron relaxation time of PCs stabilized in some solids may increase with the ω_e . This is another reason for the appearance of fast passage effects that make it possible to study efficiently their relaxation and dynamics properties. We have also shown²² that at this waveband it is possible to use the ST-EPR method in the study of anisotropic superslow molecular dynamics in organic solids. In contrast with the nitroxide radicals usually introduced as spin probes or spin labels into condensed systems, the native polarons stabilized in CPs with heteroatoms in backbone possess anisotropic magnetic parameters and, therefore, may be considered themselves as stable spin labels. The nearest environment of such PCs remains undis-

turbed, and the results obtained from the study of their molecular and dynamics properties become more accurate and complete. Besides, the sensitivity of the ST-EPR method also increases with ω_e ,^{9,23} so it can be used more efficiently in the study of the structure and macromolecular dynamics of CPs at 2 mm waveband EPR.

In the present paper the principles of the study by the 2 mm waveband ST-EPR method of electron relaxation and superslow anisotropic macromolecular dynamics are described and the results of such a study of various CPs with heteroatoms are summarized.

II. EXPERIMENTAL

In the study was used the filmlike initial regioregular Aldrich® poly(3-octylthiophene) (P3OT),²⁴ as well as the P3OT sample treated by annealing at 450 K for two hours (P3OT-A) and by recrystallized from chloroform for 2.5 h following annealing like P3OT-A one (P3OT-R). Also used were powder-like PTF samples in which TTF units are linked *via* phenyl (PTTF-Ph) or tetrahydroanthracene (PTTF-THA) bridges,²⁵ the emeraldine base form of polyaniline (PANI-EB),²⁶ and an initial poly(*bis*-alkylthioacetylene) (PATAC) irradiation by an argon ion laser at $\lambda = 488$ nm with 5 J/cm² (PATAC-1) and 20 J/cm² (PATAC-2) doses.²⁷ The samples were placed into quartz capillaries with inner diameters of approximately 0.6 mm and lengths of approximately 10 mm (an active length of the samples in site of a cavity center was only approximately 3 mm).

Registration of both the real χ' and imaginary χ'' terms of paramagnetic susceptibility χ was performed at the 2-mm (140 GHz, D-band) EPR-05 spectrometer²⁸ with 100 kHz field *ac* modulation for phase-lock detection at 90–340 K and nitrogen atmosphere. The precise MW bridge adjustment was obtained by an attainment of the symmetric first derivative of dispersion standard signal in the device output. A single crystal of dibenzotetrafulvalene platinum hexabromide, (DBTTF)₃PtBr₆ with a linear size of about 0.1 mm and $g = 2.00552$ was found to be suitable for such purpose. Modulation frequency phase was precisely adjusted by a minimum its $\pi/2$ -out-of-phase nonsaturated signal with the following phase change by $\pi/2$. In this case the $\pi/2$ -out-of-phase signal attenuation reaches more than 23 dB. Another single crystal, (fluoranthene)₂PF₆, was used for the determination of the magnetic term of RF field B_1 as described in details in Ref. 22. This value was evaluated from its EPR spectra using the steady-state saturation method of $B_1 = 0.2$ G.

III. RESULTS AND DISCUSSIONS

A. Poly(3-octylthiophene)

Figure 1(a) shows the 3 cm waveband EPR absorption spectrum of an initial poly(3-octylthiophene) sample registered at room temperature (RT). At this waveband the sample demonstrates noninformative solitary nearly Lorentzian EPR spectrum with $g = 2.0019$ and peak-to-peak line width of $\Delta B_{\text{pp}} = 2.7$ G. As the microwave frequency increases to 140 GHz, the spectrum is transformed to the superposition of

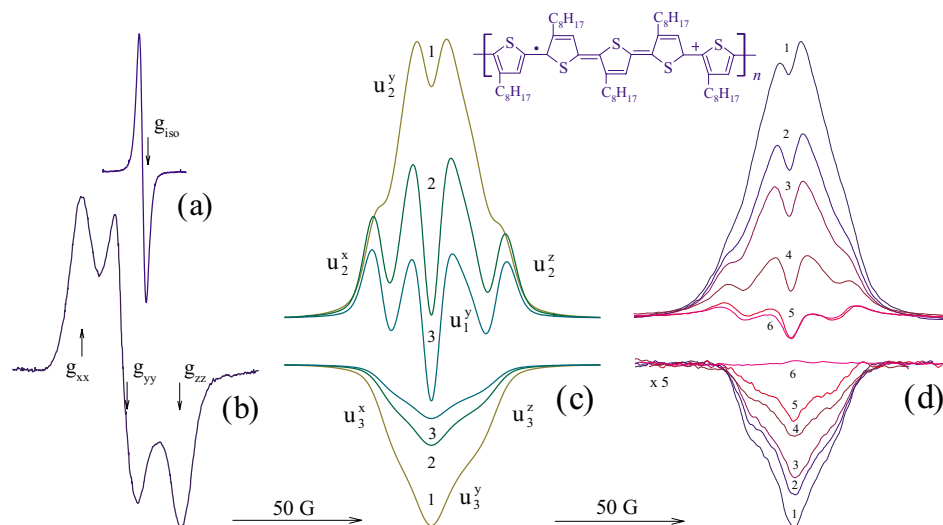


FIG. 1. (Color online) Room temperature in-phase absorption spectra of polarons diffusing in regioregular poly(3-octylthiophene) registered at 3 cm (a) and 2 mm (b) waveband EPR; (c) in-phase (above) and $\pi/2$ -out-of-phase (below) 2 mm waveband dispersion spectra of polarons obtained for $B_1=0.1$ G (1), $B_1=B_{10}$ (2), and $B_1=0.005$ G (3); (d) in-phase (above) and $\pi/2$ -out-of-phase (below) 2 mm waveband dispersion spectra of polarons registered at $T=90$ K (1), 100 K (2), 110 K (3), 145 K (4), 200 K (5), and 250 K (6). Polaron extended on three monomer units is shown schematically as well. Spin and charge density are spread out to a larger extent than shown here.

more broadened convoluted Gaussian and Lorentzian lines with an anisotropic g factor [Fig. 1(b)] as it is typical for PCs in some other conducting polymers with heteroatoms.^{19,29}

From the RT spectra of P3OT the main components of its g -tensor have been determined to be $g_{xx}=2.004\ 09$, $g_{yy}=2.003\ 32$, and $g_{zz}=2.002\ 35$. The principal x axis is chosen parallel to the longest molecular c axis, the y axis lies in the thiophene ring-ring plane, and the z axis is perpendicular to the x and y axes. The treatment of this sample by an annealing at 450 K (P3OT-A) and by both recrystallization and annealing at 450 K (P3OT-R) leads to the change of these parameters to $g_{xx}=2.004\ 04$, $g_{yy}=2.003\ 15$, $g_{zz}=2.002\ 31$ for P3OT-A and to $g_{xx}=2.004\ 02$, $g_{yy}=2.003\ 13$, $g_{zz}=2.002\ 34$ for P3OT-R. It is seen from the Fig. 1(c) that additional bell-like contributions appear in both the in-phase and $\pi/2$ -out-of-phase terms of the dispersion spectrum of polarons registered at steady-state MW saturation. This effect can be explained as follows.

Electron spins being in thermal equilibrium in an external magnetic field are distributed to energy levels according to Boltzmann's law. If this equilibrium is disturbed by the increase of the MW field, the magnetic moments of the spins relax with the spin-lattice T_1 and spin-spin T_2 relaxation times. A spin-packet shape is assigned by the following set of time characteristics: T_1 , T_2 , $(\gamma_e \Delta B_{1/2})^{-1}$, ω_m^{-1} , $(\gamma_e B_m)^{-1}$, $(\gamma_e B_1)^{-1}$, and $B_1/(dB/dt)$, where γ_e is the gyromagnetic ratio for an electron, $\Delta B_{1/2}$ is the linewidth at half-height, and ω_m and B_m are the frequency and intensity of a modulation field. The first three are stipulated by the origin of the substance, and the remaining ones are instrumental parameters. If the parameters of a spectrum registration satisfy certain inequalities, it becomes possible to analyze the behavior of a magnetization vector \mathbf{M} qualitatively. If the saturation factor $s = \gamma_e B_1 \sqrt{T_1 T_2} = \gamma_e B_1 T_{\text{eff}} \ll 1$ (here, T_{eff} is the effective relaxation time), T_{eff} does not exceed the $(\gamma_e B_1)^{-1}$ precession time of \mathbf{M} vector near \mathbf{B}_1 , so the lines of the spin packet are

described by the classic analytical expression and its signal with the ordinary first-derivative shape $g^1(\omega_e)$ is detected as the projection of \mathbf{M} on the $+X$ axis.

The saturation of spin packets is realized as the opposite condition $s \geq 1$ holds. In this case, the system comes to equilibrium again at the other end of the sweep, then \mathbf{M} is initially oriented along the $+Z$ axis, \mathbf{M} and \mathbf{B}_{eff} become antiparallel during the passage, and the signal appears as the projection of \mathbf{M} on the $-X$ axis. Thus, the signal from a single spin packet is partly registered with a $\pi/2$ -out-of-phase shift with respect to the field modulation. Hyde and Dalton argued⁹ that anisotropic motions should be better studied from the analysis of the second-harmonic $\pi/2$ -out-of-phase absorption spectra. We have shown experimentally²² that at the 2 mm waveband EPR the amplitude of the second-harmonic absorption spectrum of polarons in conducting polymers is considerably smaller than that of the first-harmonic dispersion spectrum. Besides, superslow molecular dynamics is also well reflected in 2 mm waveband first-harmonic dispersion spectra U_1^1 registered at the adiabatically fast passage²² (see below). As the PCs are fast passed by the magnetic field, two additional bell-like contributions appear in the first-derivative in-phase and $\pi/2$ -out-of-phase dispersion terms,³⁰

$$U(\omega_e t) = u_1 g^1(\omega_e) \sin(\omega_e t) + u_2 g(\omega_e) \sin(\omega_e t - \pi) + u_3 g(\omega_e) \sin(\omega_e t \pm \pi/2), \quad (1)$$

where $u_i g(\omega_e)$ are the in-phase and quadrature dispersion terms with shape $g(\omega_e)$ registered at the appropriate phase detector tuning measured at $\omega = \omega_e$.

It is obvious that $u_2 = u_3 = 0$ without MW saturation of a spin packet. With the saturation being realized, the relative intensities of the u_1 and u_3 components are defined by the relationship between the relaxation time of a spin packet and the rate of its resonance field passage. If the rate of resonance passage is high and the modulation frequency is comparable

to or higher than the effective relaxation rate T_{eff}^{-1} , the magnetic field change is too fast, and the magnetization vector of the spin system does not have time for reorientation of the \mathbf{B}_1 vector. At the adiabatic condition, $\gamma_e \omega_m \ll \gamma_e^2 B_1^2$, such a delay leads to that the spin can “see” only an average applied magnetic field, and the first derivative of a dispersion signal is mainly defined by the integral $u_2 g(\omega_e)$ and $u_3 g(\omega_e)$ terms of Eq. (1) [see Fig. 1(c)]. When the effective relaxation time is less than the modulation period but exceeds the passage rate, $\omega_m > T_{\text{eff}} > B_1 / (dB/dt)$, the magnetization vector has time to relax to equilibrium state during one modulation period; therefore, the dispersion signal of a spin packet is independent of the relationship of its resonant field and an external field \mathbf{B}_0 . The sign of a signal is defined by that from which side the resonance is achieved. In this case the $\pi/2$ -out-of-phase term of a dispersion signal is also registered as an integral function of spin-packet distribution, and the first derivative of a dispersion signal is mainly defined by the $u_1 g'(\omega_e)$ and $u_3 g(\omega_e)$ terms of Eq. (1).

The shape of the ST-EPR spectrum depends on the spin-lattice relaxation and also on the orientation of the radical rotation axis with respect to its canonical \mathbf{g} -tensor axes. For evaluation of these values the spectral parameters mainly sensitive either to τ_c or to T_1 should first be chosen for each type of anisotropic motion. It was shown^{31,32} that both the electron relaxation times of adiabatically saturated spin packets at $\omega_m T_1 > 1$ can be estimated separately from the analysis of two last terms of Eq. (1) as^{31,32}

$$T_1 = \frac{3\omega_m(1+6\Omega)}{\gamma_e^2 B_{l_0}^2 \Omega(1+\Omega)}, \quad (2)$$

$$T_2 = \frac{\Omega}{\omega_m}, \quad (3)$$

where $\Omega = u_3^y / u_2^y$, B_{l_0} is the polarizing field in a cavity center at which the condition $u_1 = -u_2$ is valid [see in-phase dispersion term 2 at Fig. 1(c)]. It is seen that the determination of the B_1 value is required for the evaluation of relatively long relaxation times. Both the relaxation times of PCs in P3OT (and in other polymers described below) were determined from Eqs. (2) and (3) in wide temperature region and are not discussed here.

Mobile and localized charge carriers are characterized by anisotropic magnetic and dynamics parameters. It is convenient to choose the ratio of the amplitudes of the canonical spectral component, involved in the frequency exchange with the other spectral components (for example, y and z components at x -anisotropic rotation), to the amplitude of the component, which is not involved in such an exchange (x component in this case) as a parameter of the first type. According to the method, superslow spin motion should lead to an exchange of y - and z -spectral components and to the diffusion of saturation across the spectrum with the average transfer rate,⁹

$$\left\langle \frac{d(\delta B)}{dt} \right\rangle = \sqrt{\frac{2}{3\pi^2 T_1 \tau_c}} \frac{\sin \theta \cos \theta (B_{\perp}^2 - B_{\parallel}^2)}{\sqrt{(B_{\perp}^2 \sin^2 \theta + E_{\parallel}^2 \cos^2 \theta)}}, \quad (4)$$

where δB is the average spectral diffusion distance, B_{\perp} and B_{\parallel} are the anisotropic EPR spectrum components arrangement along the field, θ is the angle between the directions of an external magnetic field B_0 and a molecular x axis of a radical, and B_{\perp} and B_{\parallel} are the low- and high-field spectral component arrangements along the scanning field, respectively.

If the inequality⁹

$$\tau_c^x \leq \frac{2}{3\pi^2 T_1 \gamma_e^2 B_1^4} \frac{\sin^2 \theta \cos^2 \theta (B_{\perp}^2 - B_{\parallel}^2)^2}{B_{\perp}^2 \sin^2 \theta + B_{\parallel}^2 \cos^2 \theta} \quad (5)$$

holds for a correlation time of radical rotation near the main, e.g., x axis, the well-known adiabatic condition $dB/dt \ll \gamma_e B_1^2$ can be realized for the radicals oriented by the x axis along \mathbf{B}_0 and it cannot be realized for the radicals of other orientations. This results in the elimination of the saturation of the spin packets, whose y and z axes are oriented parallel to the field \mathbf{B}_0 and consequently to the decrease of their contributions to the total ST-EPR spectrum. It is seen from Eqs. (4) and (5) that the increase in registration frequency ω_e should increase the saturation transfer rate across the spectrum and broaden the range of relaxation times measured as well. Besides, the higher spectral resolution at higher ω_e allows one to analyze the affect of microwave saturation on all spectral components. One can expect to obtain more detailed information on motion when $T_1 / \tau_c \leq 1$. Fast motion causes rapid averaging over all angles, and the details of individual random walk processes are lost, whereas the motion near the rigid lattice limit means the particle does not walk far enough to give much insight into the random walk process.

We have shown²² that the $K_{\text{mov}} = u_3^x / u_3^y$ ratio determined from the first-order dispersion (see Fig. 1) or second-order absorption spectra can be used for evaluation of the correlation time of superslow radical rotation near, e.g., x axis. The respective curves calculated at different spin-lattice relaxation time and presented in the insert of Fig. 2 demonstrate how this value changes at different spin-lattice relaxation time and rotation near own main molecular x axes at different correlation times. This allows us to determine superslow macromolecular motion in CPs with heteroatoms on backbone from their 2 mm waveband ST-EPR spectra using the semiempirical equation,^{19,20,29}

$$\tau_c^x = \tau_{c0}^x \left(\frac{u_3^x}{u_3^y} \right)^{\alpha}, \quad (6)$$

where α is a constant governed by the anisotropy of spin-orbit interactions and spin-lattice relaxation time. The pre-exponential factor τ_{c0}^x is the lowest limit for the correlation time in a respective polymer matrix.

The temperature dependence of correlation time for superslow librations of polymer chains near the main x axis is presented on Fig. 2. It is shown that the τ_c^x value determined for the P3OT and P3OT-A samples decreases with the temperature increase up to $T_c \cong 150$ K and increases above this critical temperature (Fig. 2). An opposite temperature depen-

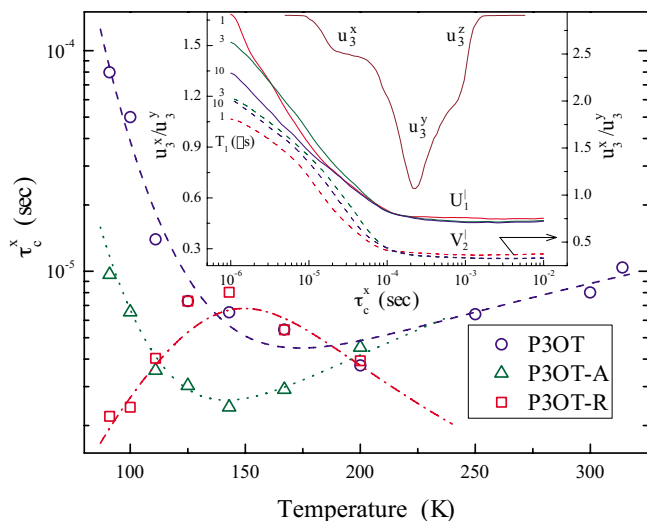


FIG. 2. (Color online) Temperature dependence of correlation time of superslow librations of macromolecules near the main x axis in the initial P3OT sample (P3OT) and in that treated by annealing at 450 K (P3OT-A), and by both recrystallization and annealing at 450 K (P3OT-R). The dependences calculated in the framework of activation motion from Eq. (8) with the data obtained for the P3OT, P3OT-A, and P3OT-R samples (see Table I) are shown by dashed, dotted, and dash-dotted lines, respectively. In the inset, the solid and dashed lines show u_3^x/u_3^y vs τ_c^x plots calculated respectively for first-harmonic dispersion U_1^x and second-harmonic absorption V_2^y spectra of PCs with $g_{xx}=2.00891$, $g_{yy}=2.00612$, and $g_{zz}=2.00267$ rotating near the x axis at different spin-lattice relaxation times T_1 .

dence with the close T_c is characteristic for P3OT-R. These dependences can be interpreted in terms of superslow activation 1D libration of the polymer chains with activation energy E_a and correlation time,

$$\tau_c^x(T) = \tau_{c0}^x \exp\left(\frac{E_a}{k_B T}\right), \quad (7)$$

(here, k_B is the Boltzmann constant) together with polarons at low temperatures when $T \leq T_c$, whereas their high-temperature part can be explained by the defrosting of collective two-dimensional (2D) motion at $T \geq T_c$. In this case, an effective correlation time is determined as

$$\tau_c^x(T) = \left[\left(\tau_{c0}^x \exp\left(\frac{E_n}{k_B T}\right) \right)^n + (k_1 T^\beta)^a \right]^{1/n}. \quad (8)$$

Figure 2 evidences that the experimental data obtained for all P3OT samples are well fitted by Eq. (8) with the constants summarized in Table I. The linear compressibility of an initial P3OT with planar chains is strongly anisotropic, being 2.5 times higher for the direction along the a axis than along its b axis.³³ It was proved that the low- and high-frequency modes exist in polythiophenes.³⁴ These modes differently su-

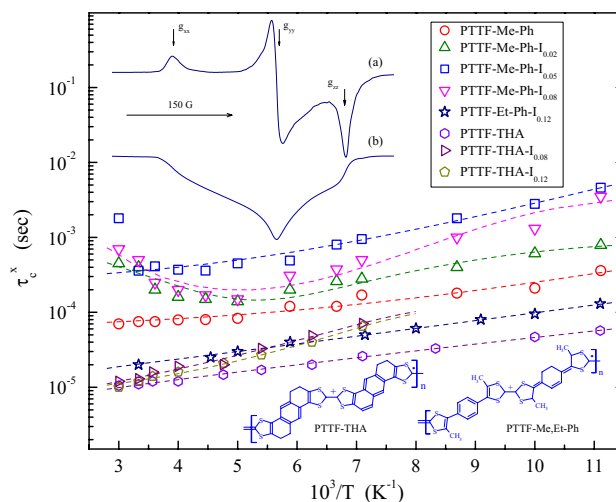


FIG. 3. (Color online) (Inset) Typical RT 2 mm waveband in-phase absorption (a) and $\pi/2$ -out-of-phase dispersion (b) EPR spectra of the initial and slightly I-doped polytetrathiafulvalene with phenyl (PTTF-Me, Et-Ph) and tetrahydroanthracene (PTTF-THA) bridges. Arrhenius dependencies of correlation time τ_c^x of x -anisotropic polaron librations evaluated from their ST-EPR spectra. The polaron is extended to a larger monomer units than shown here.

perposed in P3OT above and below T_c should lead to a change of the n exponent in Eq. (8) from 1 for “successive” macromolecular dynamics in P3OT and P3OT-A to -1 for “parallel” molecular librations in P3OT-R. Osterbacka *et al.*³⁵ have found that the interchain coupling existing in self-assembled lamellae in P3AT drastically changes the properties of the polaron excitations and that the traditional self-localized polaron in one dimension is delocalized in two dimensions, resulting in a much-reduced relaxation energy and multiple absorption bands. Therefore, the dependences obtained can indeed be interpreted in the frame of the superslow 1D libration of the polymer chains, together with polarons near their main x axis at $T < T_c$, whereas their high-temperature part can be explained by the collective 2D motion. The upper limit for the correlation time registered by the ST-EPR method for P3OT was calculated from Eq. (5) to be 4×10^{-4} s at 66 K.

B. Polytetrathiafulvalene

Typical 2 mm in-phase absorption and $\pi/2$ -out-of-phase dispersion EPR spectra of polytetrathiafulvalene registered at room temperature are presented in Fig. 3. This CPs has serum heteroatoms in the backbone (see Fig. 3), so, e.g., PTTF-Me-Ph demonstrates an anisotropic absorption EPR sum spectrum^{29,36,37} of localized PCs R_1 with slowly temperature dependent magnetic parameters $g_{xx}=2.01189$, g_{yy}

TABLE I. Preexponential factor τ_{c0}^x (in μ s), activation energy E_a (in eV) of macromolecular librations, k_1 (in 10^{-12} s $K^{-\beta}$), β , and n values calculated from Eq. (8) for the initial and modified P3OT samples.

Polymer	τ_{c0}^x	E_a	k_1	β	n
P3OT	0.013	0.069	310	1.8	1
P3OT-A	0.011	0.054	7.2	2.5	1
P3OT-R	0.063	0.073	0.31	3.5	-1

TABLE II. Pre-exponential factor τ_{c0}^x (in μs) and activation energy E_a (in eV) of macromolecular librations calculated from Eq. (7) for the PTTF samples.

Polymer	τ_{c0}^x	E_a
PTTF-Me-Ph	25	0.019
PTTF-Me-Ph-I _{0.02}	41	0.023
PTTF-Me-Ph-I _{0.05}	67	0.033
PTTF-Me-Ph-I _{0.08}	26	0.036
PTTF-Et-Ph-I _{0.12}	9.8	0.021
PTTF-THA	5.2	0.019
PTTF-THA-I _{0.08}	3.1	0.038
PTTF-THA-I _{0.12}	2.4	0.041

$=2.00544$, and $g_{zz}=2.00185$, and more mobile PCs R_2 with $g_{xx}=2.00928$, $g_{yy}=2.00632$, and $g_{zz}=2.00210$. The analogous spectrum of R_1 in PTTF-Et-Ph is characterized by the magnetic parameters $g_{xx}=2.01424$, $g_{yy}=2.00651$, and $g_{zz}=2.00235$, whereas PCs with nearly symmetric spectrum are registered at $g^p=2.00706$. The canonic components of the \mathbf{g} tensor of PCs localized in PTTF-THA are $g_{xx}=2.01292$, $g_{yy}=2.00620$, and $g_{zz}=2.00251$, whereas more mobile PCs with weakly asymmetric spectrum are characterized by the parameters $g_{\parallel}^p=2.00961$ and $g_{\perp}^p=2.00585$. These g factors exceed the corresponding magnetic parameters of the polarons in P3OT (see above), evidencing the larger interaction of an unpaired electron with sulfur nucleus in PTTF. The ratio of the concentrations of the localized and mobile PCs is 20:1 in neutral PTTF-Me-Ph, 1:1.8 in PTTF-Et-Ph, and 3:1 in neutral PTTF-THA.

As the conditions of an adiabatic saturation are fulfilled for PCs in these PTTF samples, the bell-like contributions appear in their quadrature dispersion term (Fig. 3). The analysis of this spectrum of PTTF showed the increase in the u_3^x/u_3^y ratio with temperature. As in the case of the P3OT samples, this is evidence of the saturation transfer over the ST-EPR spectrum due to superslow macromolecular libration dynamics in PTTF. Assuming activation spin motion in these CPs [Eq. (7)], the activation energy E_a values were obtained for initial and iodine-doped PTTF samples from monotonic branches of their Arrhenius curves (see Table II). One can conclude from the data presented that slight doping of the polymer doubles the activation energy of macromolecular librations in PTTF. E_a values obtained at 2 mm waveband EPR are comparable with that for interchain charge transfer in doped PTTF determined at a lower registration frequency^{38,39} that indicates the interaction of pinned and mobile polarons in this polymer matrix. The upper limit for the correlation time registered by the ST-EPR method is 1×10^{-4} s for PTTF-Me-Ph at 75 K when $K_{\text{mov}}=0.07$.

C. Polyaniline

Figure 4 shows 2 mm in-phase absorption and $\pi/2$ -out-of-phase dispersion EPR spectra of the emeraldine base form of polyaniline slightly doped with sulfuric acid. As in the case of PTTF, this sample demonstrates anisotropic sum EPR spectra of polarons R_1 localized on polymer chains and, delocalized polarons R_2 .⁴⁰ Spin density in the former is

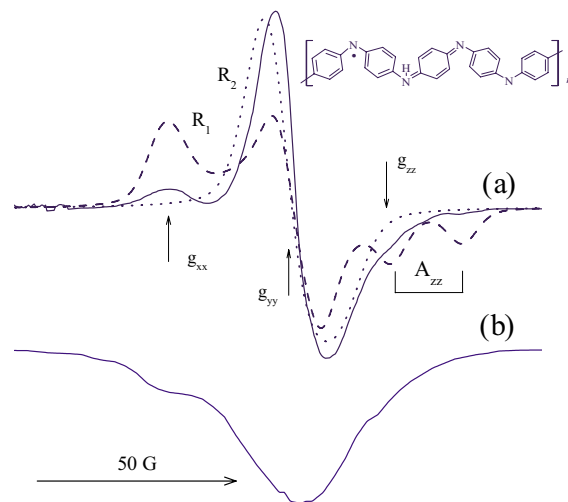


FIG. 4. (Color online) Typical RT 2 mm waveband in-phase absorption (a) and $\pi/2$ -out-of-phase dispersion (b) EPR spectra of initial and slightly I-doped emeraldine salt form of polyaniline. Dashed and dotted lines show the absorption EPR spectra calculated with $g_{xx}=2.00603$, $g_{yy}=2.00381$, $g_{zz}=2.00239$, with $g_{\perp}=2.00439$ and $g_{\parallel}=2.00376$, respectively, and $A_{xx}=A_{yy}=4.5$ G, $A_{zz}=30.2$ G.

characterized by rhombic symmetry and, therefore, by anisotropic magnetic parameters $g_{xx}=2.00603$, $g_{yy}=2.00381$, $g_{zz}=2.00239$, $A_{xx}=A_{yy}=4.5$ G, $A_{zz}=30.2$ G. An unpaired electron with axial symmetry distribution in mobile polarons R_2 is characterized by the following magnetic parameters $g_{\perp}=2.00439$ and $g_{\parallel}=2.00376$. The effective g factors of both polarons lie near one to another, i.e., $\langle g \rangle_{R1}=(1/3)(g_{xx}+g_{yy}+g_{zz}) \approx \langle g \rangle_{R2}=(g_{\parallel}+2g_{\perp})$. This indicates that radicals R_1 transform into radicals R_2 , which can be considered as a polarons diffusing along the polymer chains.

In both the in-phase and $\pi/2$ -out-of-phase terms of the 2 mm waveband dispersion EPR signal of neutral and slightly doped PANI the bell-like contribution with Gaussian spin-packet distributions is registered. The appearance of such components can also be attributed to the above-described adiabatically fast passage of the saturated spin-packets by a modulating magnetic field. The correlation time of macromolecular librations in the slightly doped polyaniline was determined from its ST-EPR spectra [Fig. 4(b)] by using Eq. (6) with $\alpha=4.8$ and Eq. (7) to be $\tau_c^x=3.5 \times 10^{-5} \exp(0.015 \text{ eV}/k_B T)$ s. Its maximum value calculated using Eq. (5) with $\theta=45^\circ$, $B_1=0.1$ G, g_{xx} and g_{yy} values measured for polaron R_1 , is equal to 1.3×10^{-4} s and corresponds to $u_3^x/u_3^y=0.22$ at 125 K.

D. Poly(bis-alkylthioacetylene)

If an initial diamagnetic PATAC is irradiated by an argon ion laser ($\lambda=488$ nm), its conductivity increases significantly and two PCs appear, namely, polarons localized on the short π -conjugated polymer chains R_1 with $g_{xx}=2.04331$, $g_{yy}=2.00902$, $g_{zz}=2.00243$, and linewidth $\Delta B_{pp}=61$ G, and polarons moving along the π -conjugated polymer chains R_2 with $g_{xx}=2.00551$, $g_{yy}=2.00380$, $g_{zz}=2.00232$, and $\Delta B_{pp}=27$ G. Analogously to the above-described CPs, the principal x axis of the spin distribution in PATAC is chosen parallel to the longest molecular c axis, the y axis lies in the C–C–

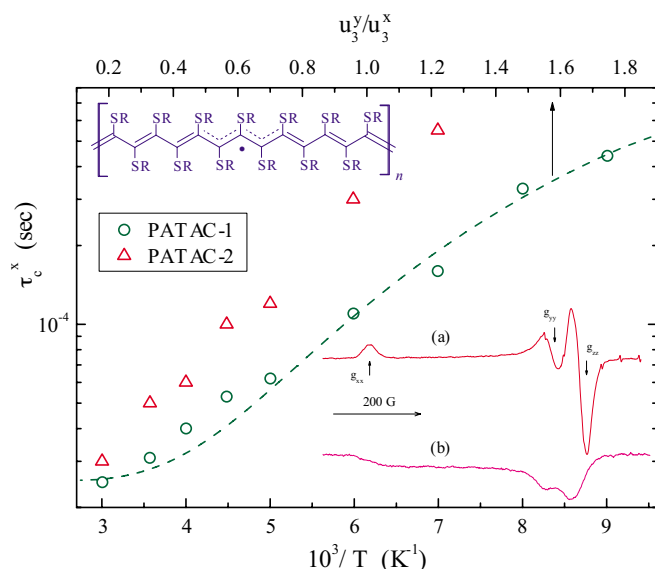


FIG. 5. (Color online) Arrhenius dependences for correlation time τ_c^x of x -anisotropic superslow librations of polarons R_1 localized in the poly(bis-alkylthioacetylene) powders irradiated by argon ion laser at $\lambda=488$ nm with different doses evaluated from their ST-EPR spectra. The dependence calculated from Eq. (6) is shown by the dashed line. In the inset are shown typical sum RT 2 mm waveband in-phase absorption (a) and $\pi/2$ -out-of-phase dispersion (b) EPR spectra of the polymer slightly treated by laser beam.

C–C plane, and the z axis is perpendicular to x and y axes. As in the case of other CPs, the averaged g factors of both polarons R_1 and R_2 lie near one to another, i.e., $\langle g \rangle_{R1} = (1/3)(g_{xx} + g_{yy} + g_{zz}) \approx \langle g \rangle_{R2}$ evidencing their identical nature and differing mobility in PATAC. Since these g factors exceed considerably the value typical for the above P3OT and PTFE also containing sulfur atoms in their own backbone, $g \approx 2.003$,²⁹ one can conclude a stronger interaction of the unpaired electrons with sulfur atoms in PATAC.

As the inequality $\omega_m T_1 > 1$ is fulfilled for the polarons in laser-modified PATAC, a bell-like contribution appears in the $\pi/2$ -out-of-phase components of their dispersion signals (Fig. 5). The heating of the laser-irradiated PATAC sample leads to the growth of the u_x^3/u_y^3 ratio due to anisotropic libration reorientations of the polymer chains with pinned polarons near the main x axis. Figure 5 presents also the correlation times of such macromolecular librations in differently laser-modified PATAC samples determined from their ST-EPR spectra. The τ_{c0}^x and E_a values in Eq. (7) were evaluated for the PATAC-1 and PATAC-2 samples from the slope of corresponding curves to be 6.3×10^{-6} s, 0.043 eV, and 3.1×10^{-6} s, 0.062 eV, respectively. The increase in the activation energy of the polymer chain librations evidences the strong dependence of the superslow macromolecular dynamics of both the pinned spins and polymer segments on the polymer treatment level. The higher the laser irradiation doses, the more rigid the polymer matrix becomes and the higher energy for the polymer chain motion is required.

IV. CONCLUSION

The data presented show the variety of electronic processes that take place in low-dimensional organic conducting

polymers, caused by the structure, conformation, packing, and degree of ordering of polymer chains, and also by the amount and the type of the dopant introduced into the polymer matrix. The higher spectral resolution and easier microwave saturation at 2 mm waveband EPR makes it possible to obtain more complete and correct qualitatively new information on magnetic, relaxation, and dynamics parameters of PCs, stabilized in conducting polymers. At this waveband, EPR spectra of polarons become more informative, interpretable and their anisotropic magnetic resonance parameters reflect the distribution of unpaired electron on nearest environment. Moreover, one succeeds in a separate determination of the times of electron relaxation of polarons in condensed systems. The 2 mm ST-EPR spectra allow one to determine the anisotropic character of the superslow macromolecular motions in conducting polymers, to define the orientation of the preferable axes of their rotation, and to estimate more accurately the characteristic times of such dynamics. The main properties of conducting polymers depend on many factors, and the advantages of the method are especially important in the identification of the structure and dynamics of such systems. The charge transfer in conducting polymers is modulated by macromolecular dynamics which, in turn, is governed by their structure, crystallinity, and treatment. This allows the establishment of the correlation between electronic and structural parameters of the polymers for controllable synthesis of various organic elements of molecular electronics with optimal properties.

ACKNOWLEDGMENTS

The author expresses his gratitude to Professor E. Fanghänel for the gift of polytetrahydrofulvalenes and poly(bis-alkylthioacetylene), Professor G. Hinrichsen for the gift of polyaniline, and Professor H.-K. Roth for fruitful discussions. Support by the Russian Foundation of Basic Researches (Grant No. 08-03-00133) and the Human Capital Foundation (Grant No. 27-02-5) is gratefully acknowledged.

¹ *One-Dimensional Metals: Conducting Polymers, Organic Crystals, Carbon Nanotubes*, edited by S. Roth and D. Carroll (Wiley-VCH, Weinheim, 2004).

² *Handbook of Conducting Polymers*, 3rd ed., edited by T. Scothorn and J. Reynolds (CRC, Boca Raton, FL, 2007).

³ Z. H. Wang, A. Ray, A. G. MacDiarmid, and A. J. Epstein, *Phys. Rev. B* **43**, 4373 (1991).

⁴ N. J. Pinto, P. K. Kahol, B. J. McCormick, N. S. Dalal, and H. Wan, *Phys. Rev. B* **49**, 13983 (1994).

⁵ S. K. Lyo, *Phys. Rev. B* **14**, 3377 (1976).

⁶ A. Madhukar and W. Post, *Phys. Rev. Lett.* **39**, 1424 (1977).

⁷ B. Ranby and J. F. Rabek, *EPR Spectroscopy in Polymer Research* (Springer-Verlag, Berlin, 1977).

⁸ H.-K. Roth, F. Keller, and H. Schneider, *Hochfrequenzspektroskopie in der Polymerforschung*, (Academic Verlag, Berlin, 1984).

⁹ J. S. Hyde and L. R. Dalton, in *Spin Labeling II: Theory and Application*, edited by L. Berliner (Academic, New York, 1979), Vol. 2, Chap. 1, pp. 1–70.

¹⁰ A. H. Beth and E. J. Hustedt, in *Biomedical EPR-Part B: Methodology, Instrumentation, and Dynamics*, edited by S. Eaton, G. Eaton, and L. Berliner (Springer, New York, 2005), Chap. 12, pp. 369–408.

¹¹ N. M. Emanuel and A. L. Buchachenko, *Chemical Physics of Polymer Degradation and Stabilization* (Science, Utrecht, The Netherlands, 1987).

¹² A. M. Wasserman and T. N. Khazanovich, in *Polymer Yearbook*, edited by R. Pathrick (Taylor & Francis, London, 1995), Vol. 12, pp. 153–184.

¹³ B. H. Robinson and L. R. Dalton, *J. Chem. Phys.* **72**, 1312 (1980).

- ¹⁴V. A. Livshits and Yu. A. Bobrov, *Vysokomol. Soedin., Ser. A* **22**, 331 (1986).
- ¹⁵T. Pali, V. A. Livshits, and D. Marsh, *J. Magn. Reson., Ser. B* **113**, 151 (1996).
- ¹⁶Ch. P. Poole, *Electron Spin Resonance* (Int. Sci. Publ., London, 1967).
- ¹⁷V. I. Krinichnyi, *J. Biochem. Biophys. Methods* **23**, 1 (1991).
- ¹⁸Y. S. Lebedev, in *Electron Spin Resonance*, edited by N. M. Atherton, M. J. Davies, and B. C. Gilbert (Royal Society of Chemistry, Cambridge, 1994), Vol. 14, Chap. 2, pp. 63.
- ¹⁹V. I. Krinichnyi, *2-mm Wave Band EPR Spectroscopy of Condensed Systems* (CRC, Boca Raton, FL, 1995).
- ²⁰V. I. Krinichnyi, in *Advanced ESR Methods in Polymer Research*, edited by S. Schlick (Wiley, Hoboken, NJ, 2006), Chap. 12, pp. 307–338; See also the website <http://hf-epr.sitesled.com/publications.htm>
- ²¹S. A. Altshuler and B. M. Kozirev, *Electron Paramagnetic Resonance of Compounds of Elements of Intermediate Groups (Russ)* (Nauka, Moscow, 1972), Vol. 2.
- ²²V. I. Krinichnyi, O. Y. Grinberg, A. A. Dubinskii, V. A. Livshits, Yu. A. Bobrov, and Y. S. Lebedev, *Biofizika* **32**, 534 (1987).
- ²³E. J. Hustedt and A. H. Beth, *Biophys. J.* **86**, 3940 (2004).
- ²⁴T. A. Chen, X. M. Wu, and R. D. Rieke, *J. Am. Chem. Soc.* **117**, 233 (1995).
- ²⁵L. V. Hinh, G. Schukat, and E. Fanghänel, *J. Prakt. Chem.* **321**, 299 (1979).
- ²⁶F. Lux, G. Hinrichsen, V. I. Krinichnyi, I. B. Nazarova, S. D. Chemerisov, and M. M. Pohl, *Synth. Met.* **55**, 347 (1993).
- ²⁷A. M. Richter, J. M. Richter, N. Beye, and E. Fanghänel, *J. Prakt. Chem.* **329**, 811 (1987).
- ²⁸A. A. Galkin, O. Y. Grinberg, A. A. Dubinskii, N. N. Kabdin, V. N. Krymov, V. I. Kurochkin, Y. S. Lebedev, L. G. Oransky, and V. F. Shuvalov, *Instrum. Exp. Tech.* **20**, 1229 (1977).
- ²⁹V. I. Krinichnyi, *Synth. Met.* **108**, 173 (2000).
- ³⁰P. R. Gullis, *J. Magn. Reson. (1969-1992)* **21**, 397 (1976).
- ³¹A. E. Pelekh, V. I. Krinichnyi, A. Y. Brezgunov, L. I. Tkachenko, and G. I. Kozub, *Vysokomol. Soedin., Ser. A* **33**, 1731 (1991).
- ³²V. I. Krinichnyi, A. E. Pelekh, A. Y. Brezgunov, L. I. Tkachenko, and G. I. Kozub, *Mater. Sci. Eng., A* **17**, 25 (1991).
- ³³J. Mardalen, E. J. Samuelsen, O. R. Konestabo, M. Hanfland, and M. Lorenzen, *J. Phys.: Condens. Matter* **10**, 7145 (1998).
- ³⁴J.-L. Sauvajol, D. Bormann, M. Palpacuer, J. P. Lère-Porte, J. J. E. Moreau, and A. J. Dianoux, *Synth. Met.* **84**, 569 (1997).
- ³⁵R. Osterbacka, C. P. An, X. M. Jiang, and Z. V. Vardeny, *Synth. Met.* **116**, 317 (2001).
- ³⁶V. I. Krinichnyi, A. E. Pelekh, H.-K. Roth, and K. Lüders, *Appl. Magn. Reson.* **4**, 345 (1993).
- ³⁷V. I. Krinichnyi, N. N. Denisov, H.-K. Roth, E. Fanghänel, and K. Lüders, *J. Polym. Sci. A* **40**, 1259 (1998).
- ³⁸H.-K. Roth, H. Gruber, E. Fanghänel, and v. Q. Trinh, *Prog. Colloid Polym. Sci.* **78**, 75 (1988).
- ³⁹H.-K. Roth, W. Brunner, G. Volkel, M. Schrödner, and H. Gruber, *Makromol. Chem., Macromol. Symp.* **34**, 293 (1990).
- ⁴⁰V. I. Krinichnyi, S. D. Chemerisov, and Y. S. Lebedev, *Phys. Rev. B* **55**, 16233 (1997).